Pediatric bone evaluation with HR-pQCT: A comparison between standard and height-adjusted positioning protocols in a cohort of teenagers with chronic kidney disease

M. Vierge, E. Preka, T. Ginhoux, R. Chapurlat, B. Ranchin, J. Bacchetta

▶ **To cite this version:**

M. Vierge, E. Preka, T. Ginhoux, R. Chapurlat, B. Ranchin, et al.. Pediatric bone evaluation with HR-pQCT: A comparison between standard and height-adjusted positioning protocols in a cohort of teenagers with chronic kidney disease. Archives de Pédiatrie, 2019, 26, pp.151 - 157. 10.1016/j.arcped.2019.02.003 . hal-03486137

HAL Id: hal-03486137
https://hal.science/hal-03486137v1

Submitted on 20 Dec 2021

HAL is a multi-disciplinary open access archive for the deposit and dissemination of scientific research documents, whether they are published or not. The documents may come from teaching and research institutions in France or abroad, or from public or private research centers.

L'archive ouverte pluridisciplinaire **HAL**, est destinée au dépôt et à la diffusion de documents scientifiques de niveau recherche, publiés ou non, émanant des établissements d'enseignement et de recherche français ou étrangers, des laboratoires publics ou privés.

Distributed under a Creative Commons Attribution - NonCommercial 4.0 International License

Version of Record: https://www.sciencedirect.com/science/article/pii/S0929693X19300272
Manuscript_f6216159ba621fdb6fa9091d6c95be80

Pediatric bone evaluation with HR-pQCT: a comparison between standard and height-adjusted positioning protocols in a cohort of teenagers with chronic kidney disease

Short title: Positioning HR-pQCT protocols in pediatrics

M. Vierge[1], E.Preka[1], T. Ginhoux[3], R. Chapurlat[2–4], B. Ranchin[1], J. Bacchetta[1–2-3–4*]

[1] Centre de Référence des Maladies Rénales Rares, Hôpital Femme Mère Enfant, 69677 Bron, France
[2] INSERM UMR 1033, Lyon, France
[3] Centre d'investigation clinique, EPICIME, Lyon, France
[4] Faculté de Médecine Lyon Est, Université Lyon 1, Lyon, France

***Corresponding author:**
Prof. Justine Bacchetta, MD, PhD
Centre de Référence des Maladies Rénales Rares
Hôpital Femme Mère Enfant
Boulevard Pinel
69 677 BRON Cedex
FRANCE
Tel: 0033–4 72 11 93 38; Fax: 0033–4 27 85 67 68
Justine.bacchetta@chu-lyon.fr

Disclosures of interest: Melody Vierge, Evgenia Preka, Tiphanie Ginhoux, Roland Chapurlat, Bruno Ranchin and Justine Bacchetta declare that they have no conflict of interest.

Acknowledgements: Institutional funding for the VITADOS cohort was provided by the Programme Hospitalier de Recherche Clinique Inter-régional (PHRCi) (J. Bacchetta, 2011). Specific funding for the local bone evaluation of pediatric CKD patients enrolled in the 4C study was provided by the Rotary Club (Ambérieu-en-Bugey, Ain, 2010). The authors would like to acknowledge the PI of the 4C study, Prof. Franz Schaefer (Heidelberg, Germany) for the coordination of the European 4C study. The authors would also like to acknowledge Dr. Stephanie Boutroy (PhD) for her scientific input.

© 2019 published by Elsevier. This manuscript is made available under the CC BY NC user license
https://creativecommons.org/licenses/by-nc/4.0/

Abstract

Background
High-resolution peripheral quantitative computed tomography (HR-pQCT) evaluates different components of bone fragility. The positioning and length of the region of interest (ROI) in growing populations remain to be defined.

Methods
Using HR-pQCT at the ultradistal tibia, we compared a single-center cohort of 28 teenagers with chronic kidney disease (CKD) at a median age of 13.6 (range, 10.2–19.9) years to local age-, gender-, and puberty-matched healthy peers. Because of the potential impact of short stature, bone parameters were assessed on two different leg-length-adjusted ROIs in comparison to the standard analysis, namely the one applied in adults. The results are presented as median (range).

Results
After matching, SDS height was −0.9 (−3.3;1.6) and 0.3 (−1.4;2.0) in patients and controls, respectively (p<0.001). In younger children (i.e., prepubertal, n=11), bone texture parameters and bone strength were not different using standard analysis. However, using a height-adjusted ROI enabled better characterization of cortical bone structure. In older patients (i.e., pubertal, n=17), there were no differences for height between patients and controls: with the standard evaluation, cortical bone area and cortical thickness were significantly lower in CKD patients: 85 (50–124) vs 108 (67–154) mm^2 and 0.89 (0.46–1.31) vs 1.09 (0.60–1.62) mm, respectively (both p<0.05).

Conclusions
Adapting the ROI to leg length enables better assessment of bone structure, especially when height discrepancies exist between controls and patients. Larger cohorts are required to prospectively validate this analytic HR-pQCT technique.

Key words: HR-pQCT, region of interest, leg length, positioning, children, chronic kidney disease

1. Introduction

High-resolution peripheral quantitative computed tomography (HR-pQCT) is a noninvasive 3D bone imaging technique, allowing an accurate *in vivo* characterization of human bone. Different components of bone fragility can be evaluated, such as compartmental densities, macroarchitecture, microarchitecture, and biomechanical properties assessed by finite element analysis (FEA) (1). However, the exact positioning and length of the region of interest (ROI) is of particular importance. In adults, the recommendations are to study a ROI located at a fixed distance from the tibial and radial endplates (1).

Yet, with fixed offset, the results are affected by the length of the bone (2), especially at the distal part where bone is subject to substantial variations in architecture and density (3). Using pQCT, a small difference in the ROI location significantly impacts the results of geometric and density parameters (4). The use of a measurement position scaled to bone length (relative measurement) shifted the ROI to as much as 3.5 mm in the axial direction when tibia length ranged from 30.8 to 39.2 cm, resulting in up to 17% variations in morphologic bone parameters (3).

This challenge in accurately positioning the ROI is even more important in growing individuals. The growth rate in children is continuous but not linear from birth to adulthood, until they reach their final adult height after the closure of the growth plates. In daily life, evaluating bone in pediatrics is challenging. First, in cross-sectional studies, two situations can be encountered: the comparison between healthy children (e.g., pubertal vs prepubertal, or boys vs girls), and the comparison between children with chronic diseases and healthy peers. Regardless of the etiology of height discrepancies between the groups, it might compromise an adequate comparison of the bone parameters with HR-pQCT. As such, the ROI could be located closer to the diaphyseal region in smaller subjects. Second, from a longitudinal study

point of view, growth itself modifies the ROI and when identical positioning is used longitudinally, the studied bone area will eventually differ.

In pediatrics, several positioning protocols have already been described with HR-pQCT. One followed the manufacturer's recommendations presented above, i.e., a ROI located at a fixed distance from the endplate, as already published by our team (5) and others (6). Others proposed a ROI set at a fixed distance from the proximal limit of the epiphyseal growth plate, determining, from radiographs for example, that a ROI in the distal radius at 7% of bone length excluded the radial growth plate in 100% of participants (7), with sometimes comparisons between techniques (8). Finally, another protocol proposed a relative position of the ROI (most distal slice: 4%–7% of the radial length and 7%–8% of the tibial length) (9). All these protocols applied an analysis on all 110 acquired slices, which appears questionable in subjects with different bone sizes. Indeed, this type of analysis leads to a proportionally larger (smaller) ROI for smaller (taller) patients, likely modifying the results.

Chronic kidney disease (CKD) is a well-known condition inducing both pubertal delay and growth retardation (10), so that the total height gain is reduced (11). Therefore, the comparison of a CKD child with a healthy peer after adjustment for traditional parameters such as gender, age, and pubertal status often leads to major discrepancies of anthropometric parameters, notably height. Conversely, if an adjustment is made on height, the healthy peer used for the comparison will be, on average, 2 years younger (12). Therefore, we believe that a pediatric population of CKD patients could be a meaningful model to evaluate analytical methods used to adjust the ROI according to the individual height.

HR-pQCT seems particularly relevant to study renal osteodystrophy (5), since it discriminates the biphasic effects of secondary hyperparathyroidism on cortical and trabecular bone (13). CKD children display an increased risk of fracture, with an annual incidence of fractures two to three times higher than in general populations (14).

The main objectives of this study were to test new methods of ROI positioning and length to take into account the individual variability of bone length and to evaluate the microarchitecture, cortical porosity, and biomechanical properties of moderate to severe CKD pediatric patients as compared to healthy peers.

2. Patients and methods

2.1.Study participants

A local subgroup of 28 pediatric patients with CKD enrolled in the European 4C study between 2010 and 2011 was evaluated (15). In addition to the 4C standard yearly evaluation, leg length, HR-pQCT at the ultra-distal tibia and additional biomarkers were assessed between 2013 and 2015. These 28 patients were matched with 28 healthy controls included in an epidemiologic cohort of teenagers designed to evaluate bone, nutritional, and cardiovascular status in healthy teenagers between 10 and 18 years of age (VITADOS cohort, NTC01832623). The matching criteria were the following: same gender, ±1 year for age (except 2 years for one pair), and ±1 for Tanner stage. The study was approved by a local independent ethics committee (Comité de Protection des Personnes Lyon Sud-Est II), and informed consent was obtained from parents before participation.

2.2.Anthropometry and physical maturity

Height and body weight were measured and expressed in standard deviation scores according to French pediatric growth charts. Tibia length was measured, the knee flexed at 90%, from the proximal margin of the medial malleolus to the proximal border of the medial tibial condyle with a tape measure by the same operator. Pubertal maturity was determined according to Tanner's staging. Patients were divided into two groups: a pre-to-early puberty group (i.e., Tanner stage I–II for at least one parameter) and a mid-to-late puberty group (i.e., Tanner stage III–V for both parameters).

2.3.Biochemical data

Calcium, phosphate, bicarbonate, and IDMS-standardized creatinine were assessed using routine techniques. Estimated glomerular filtration rate (eGFR) was calculated with the 2009 Schwartz formula. CKD stages followed the National Kidney Foundation definitions, as follows: CKD stage 3 when eGFR is between 30 and 59, stage 4 between 15 and 29, and stage 5 below 15 mL/min per 1.73 m². Intact parathyroid hormone (PTH) was measured with a second-generation assay (Roche Elecsys®, Roche Diagnosis, Mannheim, Germany, normal range: 15–65 pg/mL) and 25-OH vitamin D (25OHD) with a radio immunological technique (DIASORIN® assay, Diasorin Diagnosis, Saluggia, Italy; normal range, 50–120 pmol/L).

2.4.Bone density, microarchitecture and strength

Detailed methods for HR-pQCT analyses are available in the **Supplemental material** (Appendix 1). All subjects underwent HR-pQCT bone imaging (HR-pQCT, XtremeCT, Scanco Medical AG, Brüttisellen, Switzerland) at the ultra-distal tibia (5). The distance between the reference line and the proximal limit of the growth plate was measured in all children with open or visible growth plate by the same operator (MV). For the standard analysis, a trained operator generates semiautomatic contours around the periosteal surface; the entire volume of interest is thereafter automatically separated into a cortical and trabecular region. The outcome variables included total area (Tt.Ar, mm²); volumetric bone density (mg HA/cm^3) for the total (Tt.BMD), trabecular (Tb.BMD), and cortical (Ct.BMD) compartments; cortical thickness (Ct.Th, µm); and trabecular number (Tb.N, mm^{-1}), thickness (Tb.Th, µm), separation (Tb.Sp, µm), and intraindividual distribution of separation (Tb.Sp.SD, µm). In addition to the standard analysis, a double contouring method was applied to distinguish cortical from trabecular bone. The outcome variables included total, trabecular, and cortical area (Tt.Ar, Tb.Ar, and Ct.Ar, mm²); volumetric bone density (mg HA/cm^3) for total (Tt.BMD), trabecular (Tb.BMD), and cortical (Ct.BMD) compartments; cortical thickness (Ct.Th, mm), porosity (Ct.Po, %), and cortical pore diameter (Ct.PoDm, µm); and trabecular

number (Tb.N, mm^{-1}), thickness (Tb.Th, µm), separation (Tb.Sp, µm), and intraindividual distribution of separation (Tb.Sp.SD, µm), in the refined compartments (16). Biomechanical parameters were estimated from µFEA performed on segmented HR-pQCT images (IPL software v1.13, Scanco Medical AG) (17).

Because of the potential impact of leg length in growing children, bone density and microarchitecture were assessed in each patient and a healthy control on three different ROIs (**Figure 1**). First, the standard method, namely the full scanned ROI, corresponding to 110 axial images obtained 22.5 mm proximal to the reference line, was considered as the "Fixed offset" method. Then two other methods took into account the leg length. The second method consisted of keeping the first slice of the ROI fixed (22.5 mm proximal to the reference line), but the number of axial images was relative, depending on the leg length (relative last slice); this method was referred to as the "Fixed-rel" method (18). The third method consisted in choosing the first and last slices both relative to the leg length, so that the identified ROI began at, and spanned over, a fixed percentage of the leg length; this method was named the "Rel-rel" method.

2.5.Statistical analyses

The statistical analyses were performed using the SPSS software® 16.0 for Windows. The groups were compared using the nonparametric Wilcoxon signed-rank test. All statistical tests were performed at the two-sided 0.05 level of significance. Data are presented as median (range). The different ROI positioning protocols were compared using the percentage difference between the mean.

3. Results

3.1.General characteristics

Table 1 summarizes the anthropometric, clinical, and biological data for the CKD patients and their paired healthy controls in the two subgroups, i.e., the prepubertal and the pubertal subjects.

3.2.Differences in leg lengths between controls and patients

Leg length correlated well with height both in CKD patients and in healthy controls, as illustrated in **Supplemental Figure 1a** (Appendix 1). We therefore concluded that this parameter could be used to determine a height-dependent ROI. The range of leg length was larger in CKD patients than in controls, as summarized in **Supplemental Figure 1b** (Appendix 1); these differences were more pronounced in the prepubertal group: 30 [27–34] cm in CKD patients vs 32 [31–35] cm in healthy peers (p=0.06). In the older group, there were no differences between CKD patients and controls.

3.3.Scout-view analyses

All subjects belonging to the prepubertal group displayed a largely open growth plate. In both healthy subjects and CKD patients, the proximal limit of the epiphyseal growth plate was located 3.40 [2.73–4.41] % of the leg length above the reference line in this subgroup (**Figure 1**).

3.4. Positions of the ROI with the different positioning protocols

Using the standard technique, the first slice of the ROI was located between 6.5 and 8.3% of the leg length in the prepubertal group and between 5.6 and 7.0% in the pubertal group. Similarly, the last slice was located between 9.1 and 11.7% and between 7.9 and 9.9% of the leg length, respectively. The standard ROIs cover 2.86 [2.61–3.34] % of the leg length in the prepubertal group (Figure 1) and 2.51 [2.26–2.82] % in the pubertal group.

When using the “Fixed-rel” method, we analyzed 100% of the ROI in the tallest subject of the group (first slice fixed) and a variable length of the ROI corresponding to the percentage of

the individual length of the subject as compared to the tallest subject of the group. A median of 95 [81–104] slices were thus analyzed in the prepubertal group (89 [81–102] vs 96 [92–104] in CKD patients and controls, respectively; *p*=NS) and 94 [83–104] in the pubertal group (94 [83–104] vs 95 [86–101] slices in CKD patients and controls, respectively; *p*=NS).

When using the Rel-rel method, the first and last slices studied were relative and located at a fixed percentage of the subject's leg length. In the prepubertal group, this height-adjusted ROI was located between 8.3 and 9.1% of the leg length, and in the pubertal group between 7.0 and 7.9%. A median of 30 [25–32] slices were analyzed in the prepubertal group (27 [25–32] vs 30 [28–32] slices in CKD patients and controls, respectively; $p<0.05$) and 36 [31–29] in the older group (36 [31–39] vs 36 [32–38] slices in CKD patients and controls, respectively, *p*=NS).

3.5.HR-pQCT quantitative analysis: bone structure and FEA using the "Fixed offset" protocol

We first analyzed results of bone structure and mechanical properties obtained with the "Fixed offset" protocol. All the following results are summarized in **Supplemental Table 1** (Appendix 1).

In the prepubertal group, the median total area, cortical area, cortical thickness and cortical porosity were not different in CKD patients compared to healthy peers. There were also no significant differences between healthy controls and CKD children for bone geometry, volumetric densities, structure, and mechanical properties.

In the pubertal group, the median total area was not different in CKD as compared to healthy peers, but CKD teenagers displayed lower cortical area and thinner cortices: 86 [50–127] vs 106 [66–154] mm^2 (p=0.01), and 0.90 [0.46–1.38] vs 1.13 [0.58–1.65] mm (p=0.02), respectively. Trabecular thickness was also lower in CKD patients: 218 [179–243] vs 230 [205–252] µm (p=0.046), with no other impairment of trabecular structure. There were no

significant differences for bone volumetric density. Using FEA, CKD patients tended toward a lower estimated failure load and stiffness when compared to controls: 9100 [5483–13215] vs 9899 [6696–13124] N (p=0.082), and 386.6 [215.7–555.4] vs 425.9 [272.9–561.2] kN/mm (p=0.06), respectively.

3.6.HR-pQCT quantitative analysis: comparisons of the results obtained with the different positioning protocols

Comparisons based on the "Fixed-rel" protocol did not change the pattern previously obtained between CKD patients and controls using the "Fixed offset" protocol, as illustrated in Supplemental Table 2 (Appendix 1).

In the prepubertal group, when using the "Rel-rel" method, substantial modifications of the cortical structure were observed, as illustrated in Table 2. Between CKD patients and controls, when applying first the "Fixed offset" technique and then the "Rel-Rel method," the difference between median cortical area decreased: from 391 [337–688] to 401 [348–620] in CKD patients, and from 539 [336–685] to 497 [332–619] mm^2 in controls, therefore providing a correction for height discrepancies. As illustrated in Figure 2, the differences between the mean of the results for the total area parameter decreased from 13% with the "Fixed offset" method to 8% with the "Rel-rel" technique. Therefore this also allowed us to correct for anthropometric discrepancies and a more accurate comparison between CKD patients and controls. Interestingly, when evaluating the cortical area, the results increased from 9% to 14% (p=0.07). Similarly, the results for cortical thickness increased from 1% to 10%. Last, cortical porosity significantly decreased in CKD patients, as compared to healthy controls: 3.90% [1.60–9.0] vs 5.80% [4.60–8.40] (p=0.05), with an increased difference between the means (from 7% to 24%).

In the pubertal group, results of bone microarchitecture with the different height-adjusted ROIs are summarized in Supplemental Table 2 ("Fixed-rel") and Table 2 "Rel-rel"). In this

age group, regardless of the method, no changes in results were observed between CKD patients and controls, as also illustrated in Figure 2.

4. Discussion

In this HR-pQCT study, we demonstrated how adjusting the position and length of the ROI (using a protocol with both a relative first and last slice) to the individual leg length could be of interest when there were height discrepancies between the two groups of subjects. We showed that cortical-related parameters were significantly modified (up to 17% for Ct.Po) using a height-adjusted ROI. By applying this approach to CKD teenagers, we showed that prepubertal CKD patients presented with a significantly lower Ct.Po than healthy controls that was not observed with the standard ROI technique. Finally, we also observed a significant lower cortical area and thickness (and a trend for lower bone strength) in pubertal CKD patients.

Two main errors may be encountered from the use of the standard "Fixed-offset" positioning protocol when height (and therefore leg length) differs between subjects. First, the ROI will be more proximal in smaller subjects, and consequently more distal in taller subjects (19). Second, measurement errors can also result from the use of a fixed length for the ROI, which is proportionally larger in the shortest patients and also smaller in the tallest patients. In this study, the standard ROI covered 2.26 and 3.34% of the leg length in the smallest and tallest subjects, respectively. We therefore believe that these two potential confounding factors can lead to inaccurate results when using standard protocols to compare two groups of subjects with different heights (regardless of the quality of matching for other parameters). In that setting, we showed that the standard "Fixed offset" ROI, as compared to the "Rel-rel" ROI, underestimated the differences of cortical parameters between prepubertal CKD patients and their matched healthy peers, corresponding to the group in which height discrepancies were

the greatest. Few studies have investigated whether the position and/or the length of the ROI should be adjusted to compare individuals with different heights (20). For example, Hansen et al. used a standard and a height-matched position of the ROI at the tibia to evaluate bone structure and strength in adult women with Turner syndrome, as compared to healthy peers, the mean height in the two groups being 149 and 166 cm, respectively. Similar to our results, when using the height-matched ROI analysis, the results of cortical density, thickness, and bone strength were significantly modified (21). Cortical structure and bone strength are known to be strongly associated with bone length (22).

The two biases described above can be found in all protocols currently described for the positioning of the ROI in pediatrics. Cross-sectionally, it has been shown that the choice of the scanning protocol impacted the placement of the ROI and therefore prevented physicians from comparing the results obtained with different ROI protocols (8). Indeed, a smaller region of overlap between the ROIs obtained with different protocols will lead to significant differences in both cortical and trabecular parameters (23).

Bone structure parameters vary along bone (and thus along the ROI); the relative proportion of cortical structure increases from the distal to the proximal part of the ROI, whereas the relative proportion of trabecular structure decreases. In adults, the standard ROI located 22.5 mm from the reference line has been defined to study a metaphyseal area with both trabecular and cortical bone (3). When comparing different positioning protocols, it has been shown that cortical parameters displayed the largest percentage differences from proximal to distal slices: 25% and 19%, respectively (8). Accordingly, we found that cortical parameters were more affected than trabecular parameters when adjusting the position and length of the ROI to leg length. Therefore, it is likely that predictable measurement errors concern more the cortical than the trabecular compartment.

Nevertheless, it is debatable whether the positioning protocols should be adapted to height or leg length. Indeed, specifically in CKD patients, some authors reported a differential growth timing in the different body parts, thus inducing a body disproportion because of an early impaired growth of the leg (24). In the current study, we did not find this discrepancy, since leg length was well correlated with height in both CKD patients and controls. We believe that leg (or arm) length (in contrast to height) would enable a more accurate adjustment for the ROI, regardless the region studied.

In the current study, the use of a height-adjusted ROI seems particularly appropriate to compare prepubertal CKD patients to controls, because heights were imperfectly matched, in contrast to the pubertal group in which there were no significant height discrepancies. Therefore, one of the key results is that when using our height-adjusted method, we observed a significantly lower Ct.Po in CKD prepubertal patients as compared to controls. There is a growing interest in studying Ct.Po using HR-pQCT, due to its contribution to bone strength (25), across the lifespan (26). Given the higher risk of fracture recently described in pediatric CKD patients, one could expect them to have a greater Ct.Po (14). In the prepubertal group, we nevertheless observed opposite results. Several hypotheses could explain such apparent discrepancies. First, increased Ct.Po has been previously described in CKD adults (27) and in children on dialysis with high bone turnover (28). Ct.Po usually increased with cortical damage due to severe hyperparathyroidism (29). In this study, we probably describe different pediatric CKD populations. First, there were no dialysis patients in our group. Second, our CKD patients had satisfactory control of PTH levels, in contrast to previously published studies: while our patients displayed median PTH levels of 115 (51–337) pg/mL, the median PTH levels were 554 (433–937) pg/mL in the pediatric dialysis patients reported by Carvalho (28). In that setting, it is also interesting to keep in mind that in Wetzsteon's paper, cortical vBMD was decreased only in patients with PTH levels above the targets (13). Moreover, a

lower Ct.Po was shown in the proximal tibia of young rats receiving PTH in comparison to controls (30), suggesting that the effect of PTH on trabecular coalescence (and thus Ct.Po) in physiological growth could be site- and age-specific. Another explanation for the discrepancies observed in our CKD patients could be differences in calcium intakes. Our controls had daily calcium intake below the current guidelines of 1200 mg/day, when, in contrast, calcium supplements and calcium-based phosphate binders were largely used in our CKD patients. Yet, baseline and progressive cortical impairment in CKD has been associated with lower calcium concentration, both with pQCT (14) and histomorphometry (31). Finally, one should not forget that Ct.Po is underestimated because of the current spatial resolution of HR-pQCT (25).

Cortical bone loss in CKD has been thoroughly described, in both adults (32) and children (13). Accordingly, we found that pubertal CKD patients had a lower cortical area and thickness than healthy teenagers, regardless of the ROI studied. Moreover, trabecular impairment due to secondary hyperparathyroidism has been previously described in CKD children using HR-pQCT and histomorphometry. The pubertal group only displayed a significantly lower trabecular thickness with standard analysis that disappeared with the height-adjusted ROI. These reassuring results are probably in line with the satisfactory control of both PTH and 25OH-D levels. In view of the cortical thinning observed in the pubertal group, we expected to observe impaired mechanical properties in the CKD group. However, in this study, there was only a trend towards decreased bone strength in CKD patients. The lack of total volumetric density impairment, previously described as one of the most important bone fragility predicting factors, could explain these results (33), but we cannot rule out a lack of power due to the small number of patients.

5. Conclusion

In conclusion, assessment of bone health is challenging in pediatric populations with ongoing growth. The use of HR-pQCT in clinical pediatric practice is promising because of its noninvasiveness and its low-radiation exposure, but there are still two main problems for its accurate interpretation in these populations: there are no international guidelines for ROI positioning and no validated normative microarchitecture databases (34). With this study, we believe that we provide a potential new analytic tool to improve bone assessment in children and more generally in patients: adapting the ROI to leg length enables a better assessment of bone structure, especially when height discrepancies exist between controls and patients.

Bibliography

1. Sornay-Rendu E, Boutroy S, Munoz F, et al. Alterations of cortical and trabecular architecture are associated with fractures in postmenopausal women, partially independent of decreased BMD measured by DXA: the OFELY study. J Bone Miner Res 2007;22:425-33.
2. Schlenker RA, VonSeggen WW. The distribution of cortical and trabecular bone mass along the lengths of the radius and ulna and the implications for in vivo bone mass measurements. Calcif Tissue Res 1976;20:41-52.
3. Boyd SK. Site-specific variation of bone micro-architecture in the distal radius and tibia. J Clin Densitom 2008;11:424-30.
4. Marjanovic EJ, Ward KA, Adams JE. The impact of accurate positioning on measurements made by peripheral QCT in the distal radius. Osteoporos Int 2009;20:1207-14.
5. Bacchetta J, Boutroy S, Vilayphiou N, et al. Bone assessment in children with chronic kidney disease: data from two new bone imaging techniques in a single-center pilot study. Pediatr Nephrol 2011;26:587-95.
6. Chevalley T, Bonjour J-P, van Rietbergen B, et al. Tracking of environmental determinants of bone structure and strength development in healthy boys: an eight-year follow up study on the positive interaction between physical activity and protein intake from prepuberty to mid-late adolescence. J Bone Miner Res 2014;29:2182-92.
7. Kirmani S, Christen D, van Lenthe GH, et al. Bone structure at the distal radius during adolescent growth. J Bone Miner Res 2009;24:1033-42.
8. Cheuk K-Y, Tam EM-S, Yu FW-P, et al. A Critical Comparison Between Two Scanning Protocols of High-Resolution Peripheral Quantitative Computed Tomography at the Distal Radius in Adolescents. J Clin Densitom 2016;19:305-15.
9. Burrows M, Liu D, Perdios A, et al. Assessing bone microstructure at the distal radius in children and adolescents using HR-pQCT: a methodological pilot study. J Clin Densitom 2010;13:451-5.
10. Franke D, Winkel S, Gellermann J, et al. Growth and maturation improvement in children on renal replacement therapy over the past 20 years. Pediatr Nephrol 2013;28:2043-51.
11. Bacchetta J, Harambat J, Cochat P, et al. The consequences of chronic kidney disease on bone metabolism and growth in children. Nephrol Dial Transplant 2012;27:3063-71.
12. Griffin LM, Kalkwarf HJ, Zemel BS, et al. Assessment of dual-energy X-ray absorptiometry measures of bone health in pediatric chronic kidney disease. Pediatr Nephrol 2012;27:1139-48.
13. Wetzsteon RJ, Kalkwarf HJ, Shults J, et al. Volumetric bone mineral density and bone structure in childhood chronic kidney disease. J Bone Miner Res 2011;26:2235-44.
14. Denburg MR, Kumar J, Jemielita T, et al. Fracture Burden and Risk Factors in Childhood CKD: Results from the CKiD Cohort Study. J Am Soc Nephrol 2016;27:543-50.
15. Querfeld U, Anarat A, Bayazit AK, et al. The Cardiovascular Comorbidity in Children with Chronic Kidney Disease (4C) study: objectives, design, and methodology. Clin J Am Soc Nephrol 2010;5:1642-8.
16. Vilayphiou N, Boutroy S, Sornay-Rendu E, et al. Age-related changes in bone strength from HR-pQCT derived microarchitectural parameters with an emphasis on the role of cortical porosity. Bone 2016;83:233-40.
17. Boutroy S, Van Rietbergen B, Sornay-Rendu E, et al. Finite element analysis based on in vivo HR-pQCT images of the distal radius is associated with wrist fracture in postmenopausal women. J Bone Miner Res 2008;23:392-9.
18. Modlesky CM, Whitney DG, Singh H, et al. Underdevelopment of trabecular bone microarchitecture in the distal femur of nonambulatory children with cerebral palsy becomes more pronounced with distance from the growth plate. Osteoporos Int 2015;26:505-12.
19. Ward KA, Riddell A, Prentice A. Letter to the editor. J Clin Endocrinol Metab 2015;100:L8.
20. Adams JE, Engelke K, Zemel BS, Ward KA, International Society of Clinical Densitometry. Quantitative computer tomography in children and adolescents: the 2013 ISCD Pediatric Official Positions. J Clin Densitom 2014;17:258-74.

21. Hansen S, Brixen K, Gravholt CH. Compromised trabecular microarchitecture and lower finite element estimates of radius and tibia bone strength in adults with turner syndrome: a cross-sectional study using high-resolution-pQCT. J Bone Miner Res. 2012;27:1794-803.
22. Wetzsteon RJ, Zemel BS, Shults J, et al. Mechanical loads and cortical bone geometry in healthy children and young adults. Bone 2011;48:1103-8.
23. Shanbhogue VV, Hansen S, Halekoh U, et al. Use of Relative vs Fixed Offset Distance to Define Region of Interest at the Distal Radius and Tibia in High-Resolution Peripheral Quantitative Computed Tomography. J Clin Densitom 2015;18:217-25.
24. Zivicnjak M, Franke D, Filler G, et al. Growth impairment shows an age-dependent pattern in boys with chronic kidney disease. Pediatr Nephrol 2007;22:420-9.
25. Nirody JA, Cheng KP, Parrish RM, et al. Spatial distribution of intracortical porosity varies across age and sex. Bone 2015;75:88-95.
26. Farr JN, Khosla S. Skeletal changes through the lifespan--from growth to senescence. Nat Rev Endocrinol 2015;11:513-21.
27. Malluche HH, Mawad HW, Monier-Faugere M-C. Renal osteodystrophy in the first decade of the new millennium: analysis of 630 bone biopsies in black and white patients. J Bone Miner Res 2011;26:1368-76.
28. Carvalho CG, Pereira RC, Gales B, S et al. Cortical and trabecular bone in pediatric end-stage kidney disease. Pediatr Nephrol 2015;30:497-502.
29. Gafni RI, Brahim JS, Andreopoulou P, et al. Daily parathyroid hormone 1–34 replacement therapy for hypoparathyroidism induces marked changes in bone turnover and structure. J Bone Miner Res 2012;27:1811-20.
30. Altman AR, Tseng W-J, de Bakker CMJ, et al. Quantification of skeletal growth, modeling, and remodeling by in vivo micro computed tomography. Bone 2015;81:370-9.
31. Wesseling-Perry K, Pereira RC, Tseng C-H, et al. Early skeletal and biochemical alterations in pediatric chronic kidney disease. Clin J Am Soc Nephrol 2012;7:146-52.
32. Nickolas TL, Stein EM, Dworakowski E, et al. Rapid cortical bone loss in patients with chronic kidney disease. J Bone Miner Res 2013;28:1811-20.
33. Nickolas TL, Stein E, Cohen A, et al. Bone mass and microarchitecture in CKD patients with fracture. J Am Soc Nephrol 2010;21:1371-80.
34. Gordon CM, Leonard MB, Zemel BS, International Society for Clinical Densitometry. 2013 Pediatric Position Development Conference: executive summary and reflections. J Clin Densitom 2014;17:219-24.

Table 1: Anthropometric, clinical, and biological parameters in CKD patients and controls

	Prepubertal		Pubertal	
	Control (*n*=11)	**CKD (*n*=11)**	**Control (*n*=17)**	**CKD (*n*=17)**
Age (years)	11.1 [10.2–13]	10.9 [10.2–12.9]	15.9 [13–17.6]	15.2 [12.7–19.9]
Male gender	9 (82%)	9 (82%)	12 (71%)	12 (71%)
Tanner stage				
I	7 (64%)	6 (55%)	-	-
II	4 (36%)	5 (45%)	-	-
III	-	-	6 (35%)	3 (18%)
IV	-	-	5 (30%)	11 (64%)
V	-	-	6 (35%)	3 (18%)
Open growth plate	11(100%)	11 (100%)	9 (53%)	10 (59%)
Anthropometric data				
Height (cm)	143 [136–152]	134 [127–154]	168 [144–178]	162 [147–180]
SDS height	0.3 [−0.80 to 1.40]	−1.64 [−3.32 to 1.17]	0.3 [−1.40 to 2.0]	−0.5 [−2.70 to 1.62]
Leg length (cm)	32 [31–35]	30 [27–34]	37 [33–39]	36 [32–40]
Leg length / height	0.22 [0.22–0.23]	0.22 [0.21–0.25]	0.22 [0.2–0.23]	0.22 [0.2–0.23]
Weight (kg)	37 [26–42]	29 [23–40]	55 [33–73]	51 [35–76]
BMI (kg/m²)	18 [15–20]	15 [13–22]	20 [16–28]	19 [16–28]
Etiology of CKD	-		-	
CAKUT	-	5 (45.5%)	-	7 (41%)
ARPKD	-		-	3 (18%)
Glomerulonephritis	-	1 (9%)	-	
HUS	-		-	2 (11.7%)
Nephronophthisis	-		-	2 (11.7%)
Other diseases	-	5 (45.5%)	-	3 (17.6%)
GFR (mL/min)	117 [95–135]	29 [12–53] *	92 [78–116]	23 [12–71] *
CKD stage				
III	-	4 (36.4%)	-	3 (17.6%)
IV	-	4 (36.4%)	-	10 (58.8%)
V	-	3 (27.2%)	-	2 (11.8%)
Kidney Tx	-		-	2 (11.8%)
Biological data				
Calcium (mmol/L)	2.4 [2.2–2.5]	2.4 [2.2–2.7]	2.4 [2.2–2.6]	2.4 [2.2–2.9]
Phosphate (mmol/L)	1.4 [1.3–1.8]	1.5 [1.2–2.1]	1.4 [1.1–1.8]	1.5 [1.2–1.8]
25OHD (nmol/L)	62 [45–123]	75 [32–116]	57 [30–129]	86 [42–134] *
PTH (pg/mL)	16 [9–24]	115 [51–337] *	18 [13–24]	128 [37–236] *
HCO^{3-} (mmol/L)	25 [20–30]	23 [20–27]	27 [22–34]	22 [14–26] *
Hemoglobin (g/dl)	147 [127–147]	119 [104–136] *	147 [129–166]	12.3[9.9–14.8] *

Results are expressed as median [range] and (%)
*p<0.05 when comparing CKD children and healthy controls in both groups
SDS, standard deviation; BMI, body mass index; CAKUT, congenital abnormalities of the kidney and the urinary tract; ARPKD, autosomal recessive polycystic kidney disease; HUS, hemolytic and uremic syndrome; GFR, glomerular filtration rate (2009 Schwartz formula); Kidney Tx: kidney transplantation

Table 2: HR-pQCT results with the "Rel-rel" height-adjusted ROI

	Prepubertal			Pubertal		
	Control (*n*=11)	CKD (*n*=11)	%	Control (*n*=17)	CKD (*n*=17)	%
Slices studied (n)	30 [28–32]	27 [25–32]	*	36 [32–38]	36[31–39]	
Geometry						
Tt.Ar [mm^2]	497 [332–619]	401 [348–620]	−19%	704 [536–831]	654 [515–892]	−7%
Ct.Ar [mm^2]	79 [50–108]	68 [50–96]	−14%	108 [67–154]	85 [50–124]	−22% *
Ct.Th [mm]	0.95 [0.58–1.37]	0.79 [0.71–1.1]	−17%	1.09 [0.6–1.63]	0.89 [0.46–1.31]	−18% *
Tb.Ar [mm^2]	430 [262–522]	346 [295–549]	−20%	594 [438–762]	549 [435–794]	−8%
Density						
Tt.vBMD [mg/cm^3]	267 [220–342]	261 [207–346]	−2%	304 [224–375]	279 [170–348]	−8%
Tb.vBMD [mg/cm^3]	176 [148–225]	193 [129–269]	10%	209 [164–237]	207 [118–274]	−1%
Ct.vBMD [mg/cm^3]	714 [624–764]	707 [647–819]	−0.9%	755 [656–908]	714 [569–893]	−5%
Trabecular structure						
BVTV	0.29 [0.25–0.33]	0.30 [0.19–0.39]	6%	0.31 [0.25–0.36]	0.32 [0.21–0.4]	2%
Tb.N [mm^{-1}]	1.71 [1.6–2.1]	1.71 [1.38–2.08]	0%	1.85 [1.6–2.2]	1.87 [1.54–2.48]	1%
Tb.Th [µm]	219 [193–245]	228 [208–238]	4%	230 [206–247]	218 [179–255]	−5%
Tb.Sp [µm]	551 [441–594]	532 [429–718]	-3%	499 [417–594]	499 [342–633]	0%
Tb.Sp.SD [µm]	209 [159–239]	200 [150–359]	-4%	205 [154–261]	203 [113–282]	−1%
Cortical structure						
Ct.Po (%)	5.80 [4.6–8.4]	3.90 [1.6–9]	-33% *	3.50 [1.0–11.3]	4.10 [0.6–10.5]	17%
Ct.Po.Dm [µm]	152 [146–176]	163 [143–175]	7%	156 [133–192]	154[140–163]	−1%

Results are expressed as median [range] and differences between the median as percentage (%)
*$p < 0.05$ when comparing CKD patients and healthy controls
HR-pQCT, high-resolution peripheral quantitative computed tomography; Tt.Ar, total area; Tb.Ar, trabecular area; Ct.Ar, cortical area; Ct.Th, cortical thickness; Tt.vBMD, total volumetric bone mineral density; Tb.vBMD, trabecular volumetric bone mineral density; Ct.vBMD, cortical volumetric bone mineral density; BVTV, bone volume / total volume; TbN, trabecular number; Tb.Sp, trabecular separation; TbSpSD, heterogeneity of trabecular separation; Ct.Po, cortical porosity; Ct.PoDm, cortical pore diameter

Figures

Figure 1: Position of the different ROIs in the prepubertal group

The reference line was positioned at the tibia endplate on a scout view (example for a 27-cm leg length). The distance between the reference line and the proximal edge of the open growth plate was measured.
The positions of the different ROIs (first slice and last slice) are illustrated as the percentage of the individual leg length.
The ROI of the "Fixed offset" protocol begins 22.5 mm below the reference line, for a 110-slice analysis. The length of the "Fixed-relative" protocol was relative to the individual leg length (according to the maximum leg length observed in the pubertal group), with a fixed first slice. The ROI of the "Relative-relative" protocol was located between 8.3 and 9.1% of the individual leg length.
The ROI of the 8% tibial length protocol begins at 8% of the tibial length, on 110 slices.

Figure 2: HR-pQCT: Different positioning protocol results in CKD

Difference (in percentage) between the mean bone microarchitecture results when CKD patients are compared to healthy controls (reference to controls).
The cortical parameters are more affected than trabecular parameters when using the height-adjusted ROI.
*$p<0.05$ when comparing CKD children and healthy controls.
Each color corresponds to a different ROI positioning protocol. Black bars represent the "Fixed offset" protocol, dark grey bars represent the "Fixed-rel" protocol, and light grey bars represent the "Rel-rel" protocol.
HR-pQCT, high-resolution peripheral quantitative computed tomography; Tt.Ar, total area; Tb.Ar, trabecular area; Ct.Ar, cortical area; Ct.Th, cortical thickness; Tt.vBMD, total volumetric bone mineral density; Tb.vBMD, trabecular volumetric bone mineral density; Ct.vBMD, cortical volumetric bone mineral density; TbN, trabecular number; TbSpSD, heterogeneity of trabecular separation; Ct.Po, cortical porosity

Appendix 1: **Supplemental material**
http://www.sciencedirect.com,doi...

Figures

Figure 1:

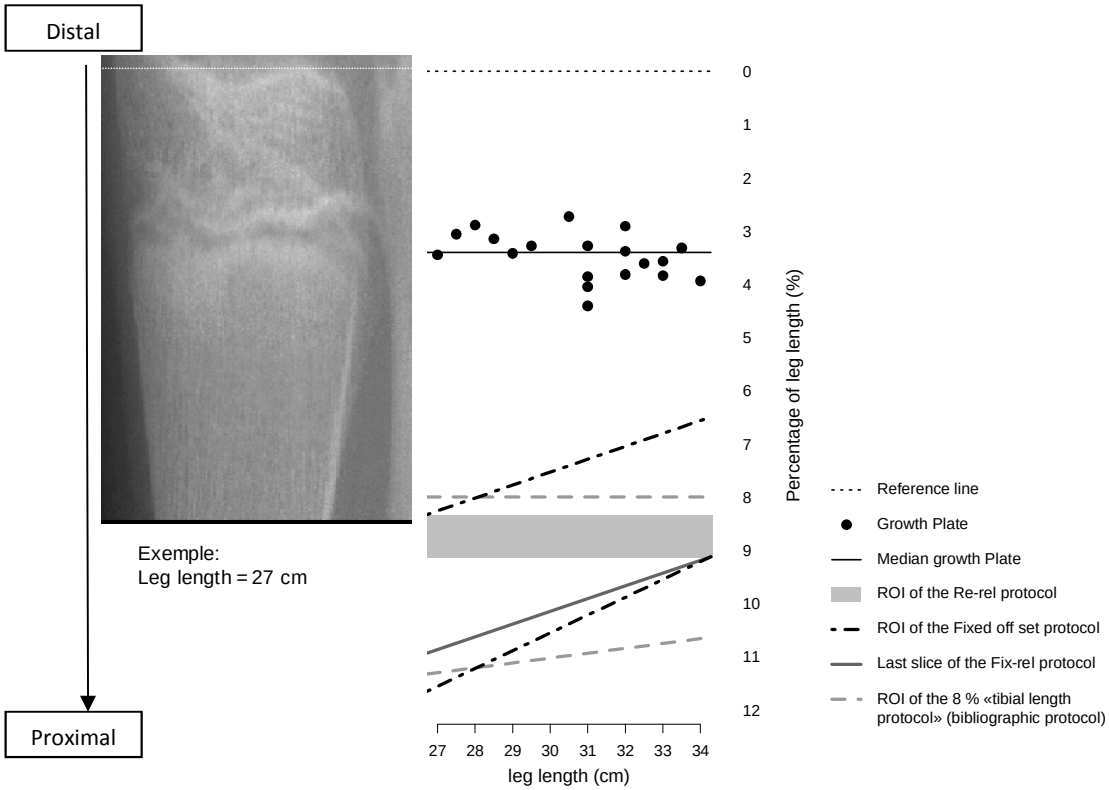

Figure 2:

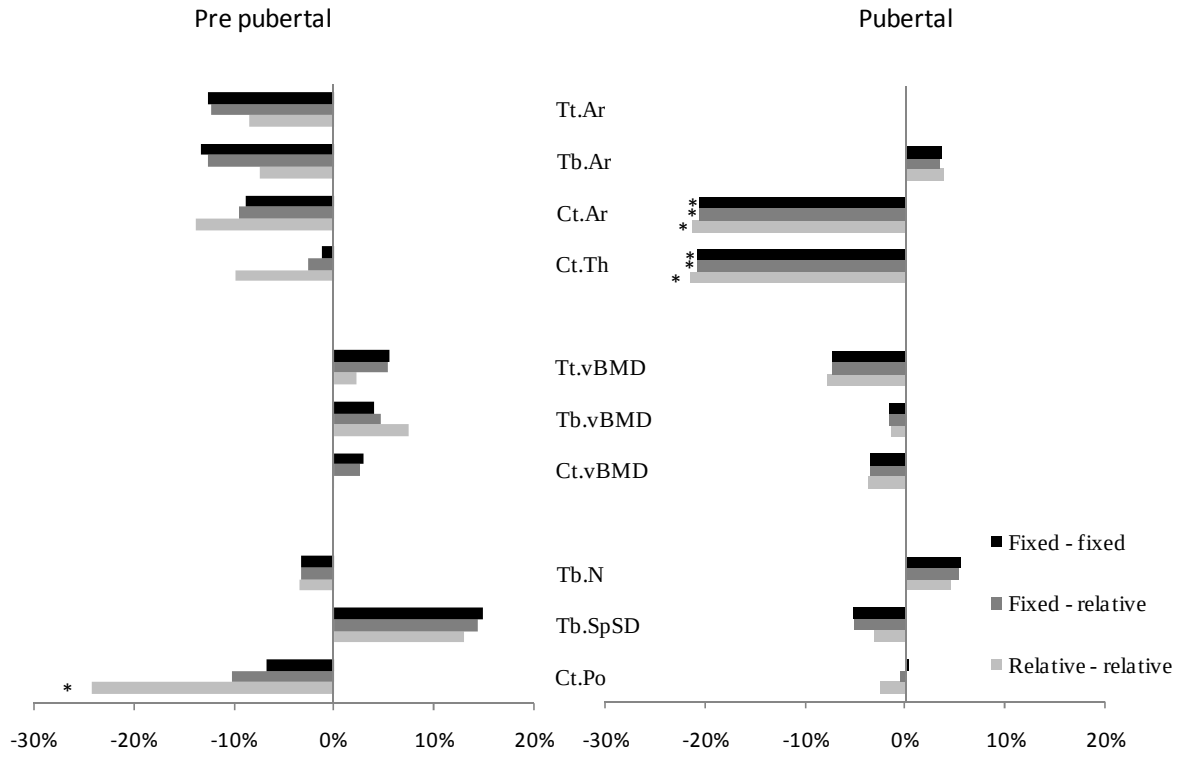
Pre pubertal
Pubertal
Tt.Ar
Tb.Ar
Ct.Ar
Ct.Th
Tt.vBMD
Tb.vBMD
Ct.vBMD
Tb.N
Tb.SpSD
Ct.Po
Fixed - fixed
Fixed - relative
Relative - relative
-30%
-20%
-10%
0%
10%
20%